1 February 1980, Volume 207, Number 4430 SCIENCE

Environmental Applications of Magnetic Measurements

R. Thompson, J. Bloemendal, J. A. Dearing, F. Oldfield
T. A. Rummery, J. C. Stober, G. M. Turner

In 1831 Faraday (1) demonstrated that movement of a magnet could produce an electric current. With the development of modern electronics, it has become possible to utilize the connection between magnetism and electricity to rapidly and easily measure many magnetic parameters of weakly magnetic natural minerals. Measurements of the magnetic properties of materials such as rocks, soils, sediments, and atmospheric particulates provide information of immense value in a wide spectrum of disciplines. The magnetic analyses are often made with a speed many orders of magnitude faster than is attainable with conventional methods of environmental analysis. This article illustrates the application of a range of rapid, simple, nondestructive, magnetic measurements to problems in geophysics, meteorology, climatology, hydrology, limnology, oceanography, sedimentology, geomorphology, soil science, ecology, and land-use studies.

Summary. A wide range of examples of the application of magnetic measurements to environmental studies illustrate the advantages of magnetic techniques over conventional methods. Magnetic measurements, in both the field and the laboratory, are particularly useful for reconnaissance work because of their speed and flexibility. Quantification as well as simple diagnosis of the transformation and movement of magnetic minerals within and between the atmosphere, lithosphere, and hydrosphere is practical. Techniques of investigating intrinsic and mineral magnetic properties, in addition to paleomagnetic remanence, are described in subjects as diverse as meteorology, hydrology, sedimentology, geophysics, and ecology.

The concentration of magnetic minerals in a sample can be estimated from its magnetic susceptibility, while the ratios between various magnetic parameters provide information about the types of magnetic grains present and their size. Concentrations of magnetic grains as low as 1 part in 10^6 can readily be measured. Although detailed and often sophisticated analyses of several properties are necessary to determine the precise magnetic composition of a sample, a wealth of information can be obtained from a few simple parameters.

Initially, we illustrate the application of three principal parameters, chosen for their diversity and speed of measurement. The first parameter, susceptibility or magnetizability, χ, can be measured on rock, soil, and sediment samples weighing 0.1 to 100 grams, on whole sediment cores, or even on exposures in the field. The air-cored coil bridge system used produces weak alternating fields (< 1 millitesla) of high frequency (~ 10 kilohertz). The second parameter, "saturation" isothermal remanence magnetization (SIRM), is measured on a sensitive magnetometer after placing a 0.02- to 20-g specimen in a strong, uniform, d-c magnetic field (1 tesla) produced by a conventional electromagnet. Only tens of seconds are needed for both the magnetization process and the remanence measurement. Several kinds of sensitive magnetometers, including flux gates, astatics, spinners, and cryogenics, are admirably suited for isothermal remanence measurement (2). The third parameter, remanent coercivity, B_{CR}—that is, the reverse d-c field required to reduce the SIRM to zero—provides a rapid method of distinguishing common natural magnetic minerals. Minerals of the corundum structure, such as hematite, have remanent coercivities above 0.2 T. Minerals of the spinel structure, such as magnetite, have remanent coercivities below 0.05 T. The B_{CR} of magnetite varies from 50 mT for grains 1 micrometer in diameter to less than 20 mT for grains exceeding 100 micrometers. Ten measurements of isothermal remanent magnetizations (IRM's), grown in increasing reverse field strengths, are sufficient to define a complete magnetization curve including the remanent coercivity.

The ratio of the first two parameters, SIRM/χ, provides a very quick first approach to monitoring the changes in magnetic mineral type or size in a suite of samples. For hematite, SIRM/χ is greater than 200 kiloamperes per meter, and for magnetite it varies from 1.5 to about 50 kA/m as the grain size decreases. Materials with a high superparamagnetic content have SIRM/χ ratios below 0.01 kA/m. Combinations of magnetic minerals in natural assemblages complicate this simple picture, but they may often be recognized by other magnetic analyses. For example, a combination of fine magnetite and ultrafine (~ 10 nanometers) superparamag-

R. Thompson is a lecturer and J. C. Stober and G. M. Turner are research students in the Department of Geophysics, University of Edinburgh, Edinburgh EH9 3JZ Scotland. F. Oldfield is a professor of geography and J. Bloemendal, J. A. Dearing, and T. A. Rummery are research students in the Department of Geography, University of Liverpool, Liverpool L69 3BX England.

0036/8075/80/0201-0481$01.25/0

netic magnetite would have a SIRM/χ ratio similar to that of coarse magnetite, but its coercivity of remanence would be higher as the ultrafine material only contributes to χ and not to the SIRM or B_{CR}.

The transformations and movement of magnetic minerals within and between the atmosphere, lithosphere, and hydrosphere are summarized in Fig. 1. The magnetic measurements outlined above can be applied to materials within all phases at or near the boundary layers. They can thus be used to identify, characterize, and quantify the transformations and fluxes portrayed. In this way, especially in view of the sensitivity of iron compounds to both natural and anthropogenic environmental processes, crucial contributions to a wide range of disciplines and to interdisciplinary studies of environmental system linkages become possible. Case studies illustrating magnetic analyses of materials from different compartments and linkages in Fig. 1 are described below.

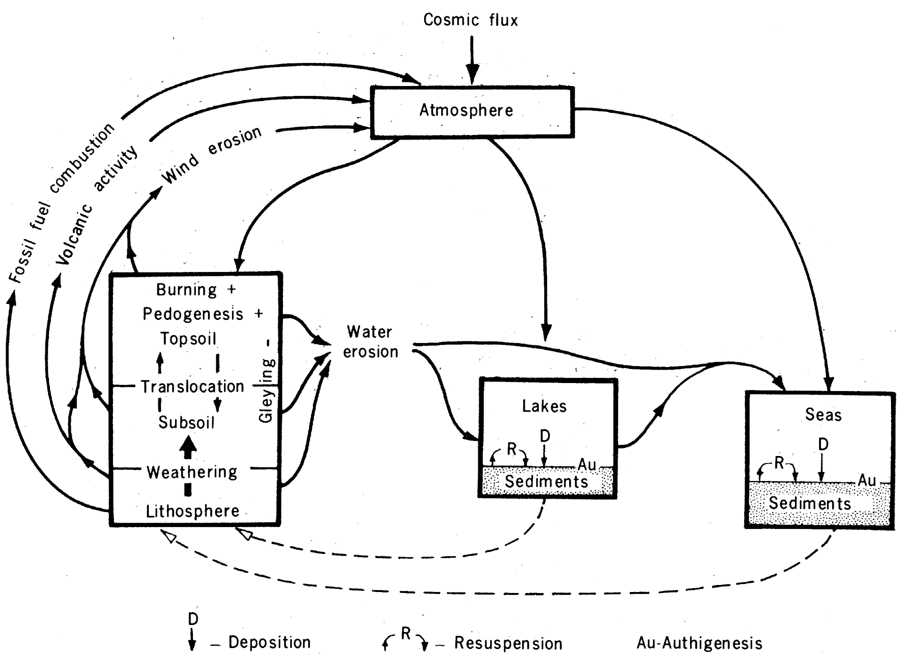

Fig. 1. Simplified model of the movements of magnetic minerals between the atmosphere, lithosphere, and hydrosphere.

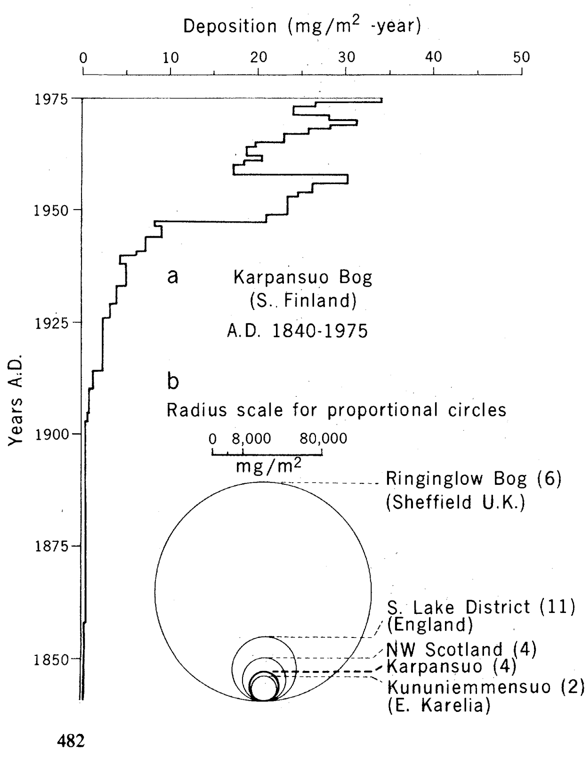

Fig. 2. Atmospheric deposition of magnetic minerals. (a) Yearly deposition of magnetite at Karpansuo Bog, Finland. (b) Spatial variation of total magnetite deposition after 1840 (after the first phase of the industrial revolution); the amount, expressed as milligrams per square meter, is represented by the area of each circle. The number of peat profiles used to calculate the post-1840 influx per square meter at each locality is shown in parentheses.

Atmosphere

Magnetic measurements provide a basis for quantifying and differentiating atmospheric particulates. Figure 2 shows atmospheric input to peat at several locations in western Europe. Time control is provided by a variety of methods (*3–5*). Where this is precise enough to allow deposition rate calculations, the results are expressed as weight of magnetite deposited per square meter per year (Fig. 2a). Not only do the profiles of SIRM versus depth or age provide a history of particulate atmospheric pollution at each site, but spatial variations in the post-1840 magnetite influx per square meter can be identified and related to the proximity of major domestic and industrial sources (Fig. 2b). In addition, B_{CR} spectra allow differentiation of the dominant source of atmospheric particulates in contemporary samples.

By applying both SIRM and B_{CR} measurements to longer peat profiles and to ice core samples, it should be possible to trace long-term qualitative and quantitative variations in particulate input. It should also be possible to identify major spatial and temporal variations in atmospheric particulate sources and compare empirical evidence with dust-veil indices reconstructed from historical records. The speed and ease with which magnetic measurements of lake sediments and peats can be used to confirm and extend correlations based on volcanic ash sequences have been demonstrated by studies of lake sediments from the New Guinea highlands (*6*).

The evidence available so far identifies anthropogenic and volcanic processes as the dominant sources of atmospheric magnetic particulates and thus has important implications for understanding the origin of magnetic minerals in deep-sea sediments. At present, these sources, together with terrestrially derived material resulting from dust storms, fires, and wind erosion, appear to predominate by orders of magnitude over the cosmic flux of extraterrestrial magnetic minerals (*3*).

Lithosphere

In many contexts, lithospheric sources of magnetic minerals predominate over atmospheric ones. Not only does the bedrock often yield primary magnetic minerals, but paramagnetic or weakly magnetic forms of iron, weathering out of parent material, may be transformed to persistent ferrimagnetic forms by fire or more gradual soil formation processes

(*7-10*). These transformations are most readily detected as an increase in χ at or near the soil surface. A firmer basis for this has been established by B_{CR} curves from topsoil and parent material from a variety of bedrock types. The ferrimagnetic minerals formed by "enhancement" in the soil have been identified by x-ray diffraction, thermomagnetic measurements, and Mössbauer effect studies as either impure maghemite (*11*) or nonstoichiometric magnetite (*9*). The downprofile variations in magnetic properties and their spatial variations provide evidence for previous forest fires (*9, 10*), land-use history (*7, 12*), and soil erosion (Fig. 3) on a wide range of parent materials.

It follows that magnetic measurements can often be diagnostic of the source of particulates once these pass into the drainage system of an area. Identifying the source of stream-borne particulates has proved difficult by nonmagnetic

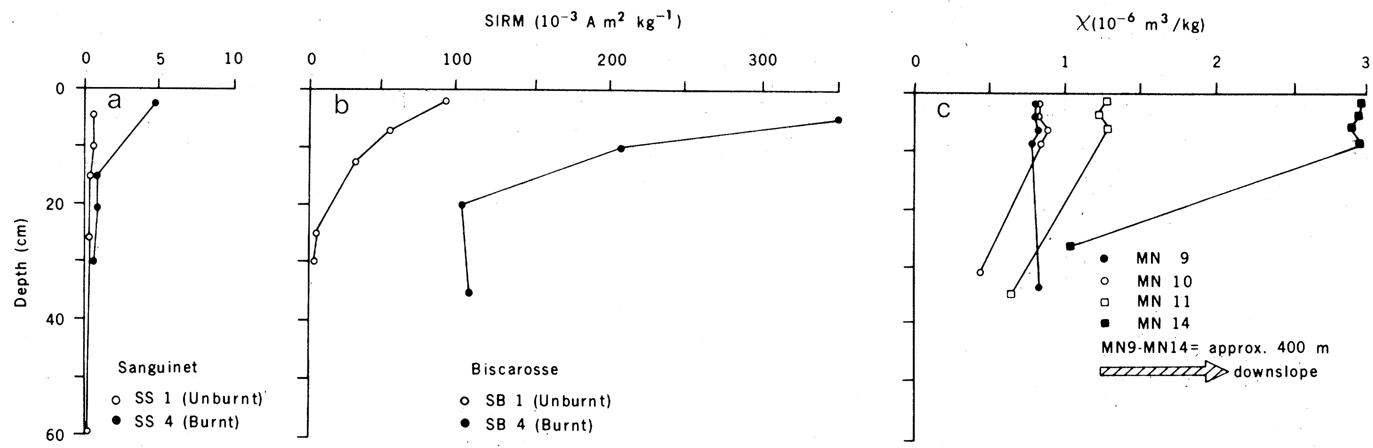

Fig. 3. Down soil profile magnetic variations for three localities in France. (a and b) Plots of SIRM against depth for burnt and unburnt profiles on Quaternary outwash sands in the Landes region. Note the enhancement of SIRM by production of ferrimagnetic minerals caused by burning. (c) Plot of χ against depth for profiles on a cultivated hillside on Jurassic limestone bedrock at Le Bois in the Montmin Valley near Annecy. The enhancement of susceptibility from the near-zero values of bedrock depends on position on the slope and land use.

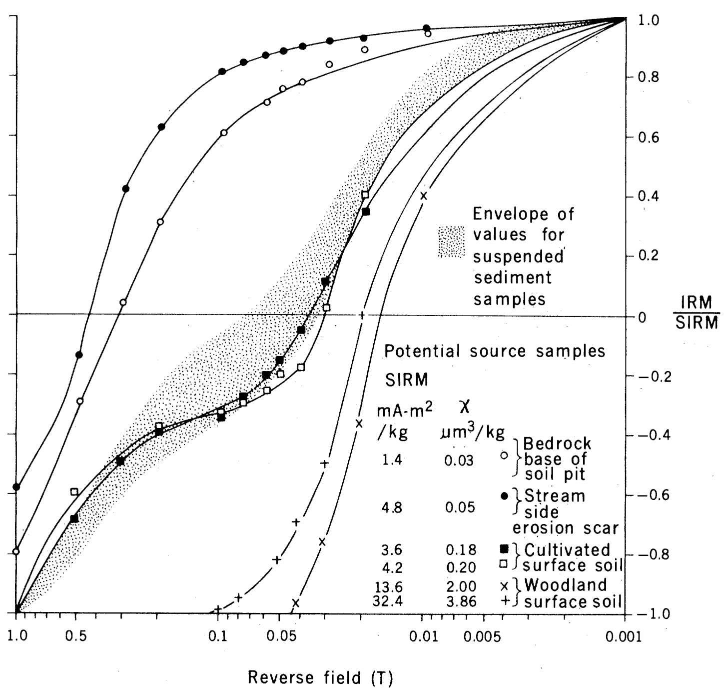

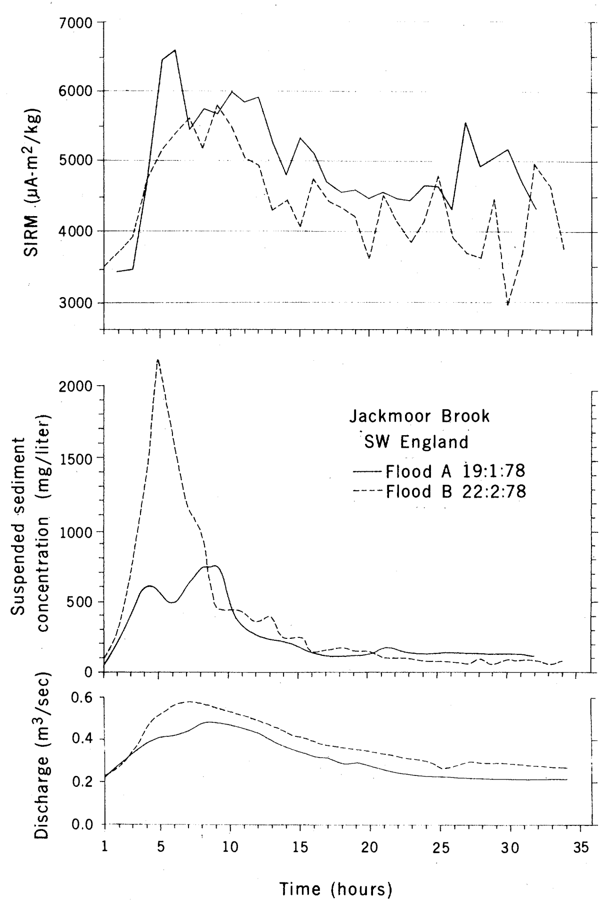

Fig. 4 (left). Coercivity of remanence spectra of bedrock, soils, and suspended sediments from an instrumented catchment in southwestern England. Note the similarity of the suspended sediment spectra to those of cultivated surface soils and their contrast with those of bedrock and woodland topsoils. Fig. 5 (right). Variation in SIRM of suspended sediment during two floods of Jackmoor Brook. Note the increase in SIRM at the time of increased runoff and sediment concentration and the lag in peak SIRM values compared with the hydrograph. This pattern is consistent with some channel scour during the rising stage of the hydrograph followed by increasing importance of surface runoff.

methods since the techniques available for differentiating materials yielded by contrasting processes such as topsoil erosion or channel scour are costly and time-consuming. Figures 4 and 5 show how, in an instrumented catchment in southwestern England, the dominant source of suspended sediment can be identified magnetically not only in a general way (*13*), but with a degree of temporal resolution that permits some estimation of the relative importance of different sources at different stages within a single flood event and at the comparable stage between flood events. This approach facilitates potentially highly sophisticated analyses of sediment type and yield, with significant implications for the study of soil loss, channel morphology, and water quality.

River-borne sediments can be traced by using the magnetic enhancement generated by either natural forest fires or artificial heating in a reducing environment in the laboratory (Table 1). The enhanced ferrimagnetic material can be used as an artificial tracer not only for suspended sediment but also for bed load, which is often exceptionally difficult to trace effectively by established techniques. With an artificially enhanced tracer, downstream dilutions of 1 part in 500 can be detected on 100-g bed-load samples with portable susceptibility bridges, or even on bed load in situ with metal detectors of the type used by treasure hunters. The insight into storage and delivery rates arising from such studies is important for studies in fluvial geomorphology and hydrology.

Lakes

Where the magnetic minerals yielded by erosion from a catchment contribute to the sediment of a lake, the down-profile variation in magnetic properties provides a rapid basis for core correlation and for the quantification and characterization of sediment influx (*12*). Figure 6 illustrates such core correlations based on magnetic whole-core volume susceptibility (κ) scanning for ten cores from Loch Lomond. Clear correlations between sediments from shallow (AIM8) and deep (TOM4) water are found, as well as between cores from near the head (GUM19) and the outflow (RPM1) of the loch. Cores GUM19 and RPM1 are more than 20 kilometers apart, separated by a pronounced trench extending to 200 m below sea level and a chain of islands with a narrow threshold of only 10-m water depth.

Magnetic measurements may also be used to date recent sediments (*14–16*). As an example, magnetic dating of these widely separated Lomond cores is based on magnetic declination measurements (*16*) (Fig. 7). These paleomagnetic direction variations are a signature of ancient geomagnetic field direction changes, which were locked into the sediment close to the time of deposition. The locking process in Lomond is due to physical stabilization of single-domain magnetite grains with diameters on the order of 1 μm. This process of postdepositional remanent magnetization involves grains that had a natural remanence before their deposition. Another possible remanence process is one in which authigenic grains acquire a fresh magnetization, in the ambient geomagnetic field direction, by growing through a critical volume. For spherical magnetite grains this critical blocking diameter is about 30 nanometers.

The stable remanence directions (Fig. 7) have been used to date the sediment by matching the oscillations with a master geomagnetic secular variation curve. In Britain three types of master curve have been used. First, the most recent secular changes have been recorded at magnetic observatories. Records at London began in A.D. 1576. Magnetic declination moved from 11°E, as recorded by Sir Martin Frobisher at that time, to 0°E in A.D. 1660. King Charles II, among others, noted the zero declination (*17, 18*). The horizontal direction continued to change and passed through a westerly maximum of 24° in A.D. 1815, while it is now about 7°W and changing much more slowly (*18*). Second, the observatory record has been extended back to A.D. 1000 by archeomagnetic studies (*19*). Paleomagnetic records for before A.D. 1000, dated by palynological changes and carbon-14 age determinations, provide a third type of master curve. The A.D. 1815 westerly maximum of the observatory records can be recognized in all the Lomond cores (Fig. 7). Lower-

Table 1. Enhancement in natural stream bed load. Material was "toasted" in a muffle furnace for 30 minutes. Note the enhancement in different particle-size fractions. Enhancement of SIRM begins to occur in fine fractions before 200°C with growth of hematite; with combustion of organic matter at higher temperatures, magnetite begins to be produced.

Size range (mm)	Natural		200°C		800°C		Enhancement	
	χ (10^{-6} m^3/kg)	SIRM (10^{-3} A m^2 kg^{-1})	χ (10^{-6} m^3/kg)	SIRM (10^{-3} A m^2 kg^{-1})	χ (10^{-6} m^3/kg)	SIRM (10^{-3} A m^2 kg^{-1})	$\frac{\chi_{800}}{\chi_0}$	$\frac{SIRM_{800}}{SIRM_0}$
<0.5	0.07	0.17	0.08	0.42	23	73	350	440
0.5– 0.7	0.07	0.13	0.08	0.58	20	55	300	430
0.7– 1.4	0.07	0.07	0.07	0.13	18	45	260	650
1.4– 2.8	0.07	0.04	0.06	0.02	15	33	230	840
2.8– 5.6	0.07	0.02	0.07	0.02	13	28	210	1200
5.6–11.2	0.07	0.02	0.07	0.02	14	33	250	1400
>11.2	0.08	0.02	0.07	0.02	16	29	230	1200

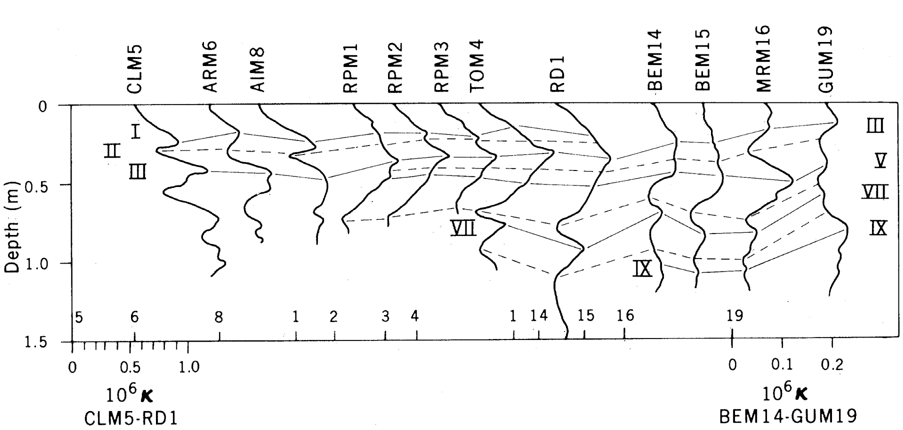

Fig. 6. Whole-core susceptibility traces for surface cores from Loch Lomond, Scotland. The locality code and number are given for each core (for example, CLM5). Susceptibility maxima are identified by odd Roman numerals and joined by solid lines. Susceptibility minima have even Roman numerals and are joined by dashed lines. The origin of the susceptibility scale for each core trace is indicated by a vertical tick on the lower axis and identified by the core number (6 refers to core ARM6). The susceptibility scales for cores CLM5 through RD1 and cores BEM14 through GUM19 are also given on the lower axis.

amplitude fluctuations of the archeomagnetic record (*19*) can also be distinguished, and the easterly turning point (D), dated at 1000 years ago, is also present in all the longer Lomond sequences. The κ variations of Fig. 6 match and reinforce the magnetic dating correlations. The speed of whole-core remanence measurements (10 centimeters per minute) (*20*) makes them very attractive when many cores are to be dated.

Extension of the whole-core magnetic correlation and dating technique to a grid spanning a whole lake makes accurate measurements of total sedimentation in a closed basin practical for the first time. Bloemendal *et al.* (*21*) illustrate this with data from a 130-core grid obtained from the sediment of Llyn Goddionduon, northern Wales, during a 2-week spell of fieldwork. Whole-core κ sensing was completed and the results were plotted in graphical form during the same period at temporary laboratory facilities close to the lakeside. Correlation of the profiles, using additional magnetic parameters, together with pollen and radiometric dating (^{14}C, ^{137}Cs, and ^{210}Pb), provides a rapid basis for quantifying material input to the sediments on a whole-lake basis. This, in turn, can be more realistically related to whole-catchment denudation than results based on extrapolation from a few cores analyzed by conventional, time-consuming methods.

Since the fluctuations in susceptibility result from changes in the concentration of magnetic minerals, they provide a basis not only for core correlation but for sedimentological interpretations, as heavy minerals, including magnetite, are sorted during transport and concentrated in sediments according to their hydrological properties. For example, in Loch Lomond magnetic concentration is related to the particle size of the sediment (*22*). The coarse silt fraction has a low concentration of magnetite, thus coarser, silty horizons are associated with low susceptibility values. The changes in particle size distributions result from environmental changes in the drainage basin—for example, variations in the relative importance of erosion of topsoil. This Lomond model of bulk susceptibility fluctuations helps to account for the linkage, first observed in Lough Neagh, between changes in pollen indicators of human activity (such as grasses, bracken, and plantains) and the susceptibility of limnic deposits (*23*).

In many lakes with catchments dominated by bedrock as diverse magnetically as ferrimagnetic-rich basalt and diamagnetic limestone, a strong direct link, similar to that observed in Loch Lomond and Lough Neagh, has emerged between the increased concentration of ferrimagnetic minerals in the sediment and accelerated erosion resulting from forest clearance and farming. In each of these cases, the most likely explanation for the link involves a shift from a sedimentation regime dominated by channel-derived material to one in which the supply from channel sources becomes relatively less important as loosened and exposed surface material transported by overland flow becomes increasingly significant. Wherever reliable time control is available (and this is coming increasingly from paleomagnetic direction measurements), acceleration in dry mass sediment accumulation accompanies the assemblage of evidence for human impact and soil loss.

Although the pattern of magnetic concentration and composition in a lake sediment is produced by local land-use variations, an underlying regional pattern can be discerned. For example, three Finnish lakes (Fig. 8, a to c) and one lake from southern Sweden (Fig. 8d) show a similar pattern of steadily decreasing magnetic concentration during the last 9000 years. In contrast, British records (Fig. 8, e to g) show much more within-core variation and more pronounced increasing concentration trends over the last 5000 years. These differences in ferrimagnetic mineral concentration between Scandinavian and British postglacial sites would become greater if the rates of sediment accumulation were taken into account and viewed in terms of the weight, or volume, of ferrimagnetic minerals accumulated per square meter per year (a flux density). This further exaggeration would arise because the χ peaks occur at times of high accumulation rate. We account for the pattern of Scandinavian χ variations as resulting from processes associated with interglacial maturation of soils and vegetation in the absence of man, as described by Mackereth (*24*), coupled with a declining allochthonous contribution to the lake sediments until very recent land-use changes, such as forest clearance and settlement, caused χ to rise again. Greater disturbance of the landscape in Britain by man, particu-

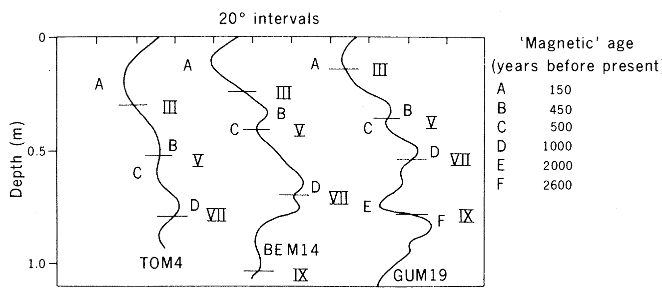

Fig. 7. Whole-core relative declination logs for three surface cores from Loch Lomond, Scotland. The susceptibility maxima from Fig. 6 are shown as short horizontal bars and confirm the correlations of the relative declination logs. The magnetic ages correspond to the declination turning points *A* to *F*.

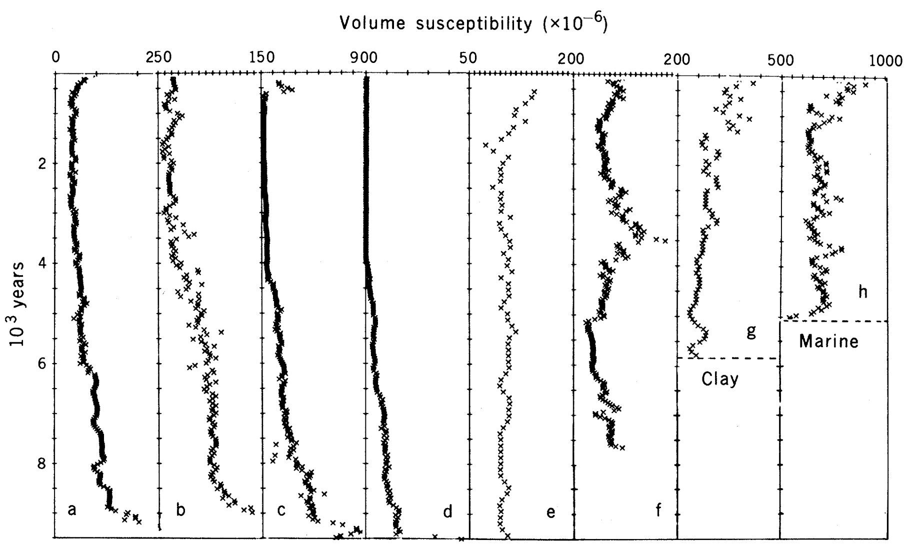

Fig. 8. Volume susceptibility logs for four Scandinavian and four British lake sediment cores: (a) Paajarvi, (b) Ormajarvi, (c) Vuokonjarvi, (d) Hjortsjon, (e) Lake Windermere, (f) Lough Catherine, (g) Lough Neagh, and (h) Loch Lomond.

larly after the decline of the elms (*Ulmus*) (*25*), would similarly account for the more variable magnetic record.

Climatic Shifts

On a longer time scale, the magnetic mineral types and concentrations reflect the weathering, pedogenic, and denudational regimes prevailing through the major climatic shifts of the Pleistocene. Magnetic measurements can provide rapid insight into the nature of these shifts, their effect of weathering, soil development, and erosion rates, and their expression in the sedimentary record. Preliminary studies confirm paleoclimatic linkages in environments as diverse as northwest England (*26*), tropical Africa, and northern Queensland (*27*). The time scales of variation differ by an order of magnitude and the climatic regimes reflected span the range from arctic-alpine to humid tropical.

Prospect

Laboratory magnetic analyses have been shown to have many applications to a wide range of disciplines associated with environmental problems. The importance of these magnetic techniques will probably be further extended by the development of sensitive instruments capable of measuring, in the field, both magnetic remanence and magnetic susceptibility.

References and Notes

1. M. Faraday, *Philos. Trans. R. Soc. London* (1832), pp. 125-162.
2. D. W. Collinson, *Rev. Geophys. Space Phys.* **13**, 659 (1975).
3. F. Oldfield, R. Thompson, K. E. Barber, *Science* **199**, 679 (1978).
4. F. Oldfield, P. G. Appleby, R. S. Cambray, J. D. Eakins, K. E. Barber, R. W. Battarbee, G. R. Pearson, J. M. Williams, *Oikos* **33**, 40 (1979).
5. P. Pakarinen and K. Tolonen, *Suo* **28** (pt. 1), 19 (1977).
6. R. Thompson and F. Oldfield, *Phys. Earth Planet. Inter.* **17**, 300 (1978).
7. E. Le Borgne, *Ann. Geophys.* **11**, 399 (1955).
8. C. E. Mullins, *J. Soil Sci.* **28**, 223 (1977).
9. G. Longworth, L. W. Becker, R. Thompson, F. Oldfield, J. A. Dearing, T. A. Rummery, *ibid.* **30**, 93 (1979).
10. T. A. Rummery, J. Bloemendal, J. Dearing, F. Oldfield, R. Thompson, *Ann. Geophys.* **35**, 103 (1979).
11. G. Longworth and M. S. Tite, *Archaeometry* **19**, 3 (1977).
12. F. Oldfield, *Prog. Phys. Geogr.* **1**, 460 (1977).
13. ——, T. A. Rummery, R. Thompson, D. E. Walling, *Water Resour. Res.* **15**, 211 (1979).
14. D. Ninkovitch, N. D. Opdyke, B. C. Heezen, J. H. Foster, *Earth Planet. Sci. Lett.* **1**, 476 (1966).
15. N. D. Opdyke, *Rev. Geophys. Space Phys.* **10**, 213 (1972).
16. F. J. H. Mackereth, *Earth Planet. Sci. Lett.* **12**, 332 (1971).
17. L. A. Bauer, *Phys. Rev.* **3**, 34 (1899).
18. S. R. C. Malin and E. C. Bullard, in preparation.
19. M. J. Aitken, *Philos. Trans. R. Soc. London Ser. A* **269**, 77 (1970).
20. L. Molyneux, R. Thompson, F. Oldfield, M. E. McCallan, *Nature (London)* **237**, 4 (1972).
21. J. Bloemendal, F. Oldfield, R. Thompson, *ibid.* **280**, 50 (1979).
22. R. Thompson and D. J. Morton, *J. Sediment. Petrol.* **49**, 801 (1979).
23. R. Thompson, R. W. Battarbee, P. E. O'Sullivan, F. Oldfield, *Limnol. Oceanogr.* **20**, 687 (1975).
24. F. J. H. Mackereth, *Philos. Trans. R. Soc. London Ser. B* **250**, 165 (1966).
25. H. Godwin, *History of the British Flora* (Cambridge Univ. Press, Cambridge, ed. 2, 1975).
26. F. Oldfield, J. Dearing, R. Thompson, S. E. Garret-Jones, *Pol. Arch. Hydrobiol.* **25**, 321 (1978).
27. A. P. Kirshaw, *Nature (London)* **251**, 222 (1974).

Disorders of Human Hemoglobin

Arthur Bank, J. Gregory Mears, Francesco Ramirez

The human hemoglobin system is a model for the study of the regulation of specific eukaryotic genes (*1*). The complete structure of the major normal human globins is known, and a variety of mutant hemoglobins have led to extensive genetic and structural analysis. A group of anemias, the thalassemia syndromes, provide a series of mutants in which the biosynthesis of either α or β globin is decreased or absent. At least some of these anemias appear to be due to defects in the regulation of structurally normal globin genes. Restriction endonuclease analysis of cellular DNA and the cloning and sequencing of human globin genes have permitted detailed analysis of the organization and structure of normal and abnormal human globin genes. These techniques have provided a linear physical map of nucleotide sequences showing the organization of these genes. Deletions of specific nucleotide sequences, both within and surrounding the human globin genes, occur in certain anemias, and regions of DNA which may be important in regulating globin gene expression have been identified. Direct analysis can now be made of the relation between changes in gene structure to alterations in gene function; also prenatal diagnosis of certain disorders of man is now possible by analysis of deletions and base substitutions in fetal DNA from cells from amniotic fluid. In this article, we review normal and abnormal human hemoglobin synthesis, and focus on the insights provided by recent studies on the regulation of the human globin genes at the molecular level.

Dr. Bank is professor of medicine, and of human genetics and development, at Columbia University College of Physicians and Surgeons, New York 10032. Drs. Mears and Ramirez were formerly research associates at Columbia University. Dr. Mears is now an assistant professor of medicine at Albert Einstein College of Medicine, Bronx, New York 10461. Dr. Ramirez is now an assistant professor in the Department of Obstetrics and Gynecology at Rutgers University Medical School, Piscataway, New Jersey 08854.

Normal Hemoglobin Biosynthesis

The major hemoglobin genes and their protein products are shown in Fig. 1. There is strong genetic and biochemical evidence for linkage of four genes other than the α genes: two γ genes, one δ gene, and one β gene on chromosome 11 (*2*). The α genes are on chromosome 16, and appear to be duplicated (*3*). Two types of γ globin genes are identified on the basis of two structural γ globins, $^G\gamma$ and $^A\gamma$, differing from each other by one amino acid. $^G\gamma$ globin contains a glycine at position 136, whereas $^A\gamma$ globin has an alanine at that position. The most stable hemoglobins are tetramers consisting of two α globins and two other globins. The two types of γ globins combine with α globins to form fetal hemoglobin (designated hemoglobin F, HbF, or $\alpha_2\gamma_2$), the major hemoglobin of the fetus; hemoglobin A (HbA, or $\alpha_2\beta_2$) is the major normal adult hemoglobin. Hemoglobin A_2 (HbA_2, or $\alpha_2\delta_2$) is another adult hemoglobin, but is produced at a low level throughout adult life. Two embryonic globin genes, the ζ and ϵ genes, are also identifiable in the fetus, and are part of the embryonic hemoglobins Gower I ($\zeta_2\epsilon_2$), Gower II ($\alpha_2\epsilon_2$), and Portland ($\zeta_2\gamma_2$) (*1, 4*). The chromosome location of the ζ and ϵ genes is unknown. The molecular events responsible for the switches from embryonic to fetal hemoglobin and from fetal to adult hemoglobin production are also unknown.